Advances in Computational Design, *Vol. 2, No. 3 (2017) 123-141*
DOI: https://doi.org/10.12989/acd.2017.2.3.123

A novel approach to the form-finding of membrane structures using dynamic relaxation method

S. Fatemeh Labbafi[1a], S. Reza Sarafrazi[1b], Hossein Gholami[1c] and Thomas H.-K. Kang[*2,3]

[1]Department of Civil Engineering, University of Birjand, Birjand, Iran
[2]Department of Architecture & Architectural Engineering, Seoul National University, Seoul, Korea
[3]Department of Civil and Environmental Engineering, University of Illinois at Urbana-Champaign, USA

(Received March 8, 2017, Revised March 27, 2017, Accepted April 10, 2017)

Abstract. Solving a system of linear or non-linear equations is required to analyze any kind of structures. There are many ways to solve a system of equations, and they can be classified as implicit and explicit techniques. The explicit methods eliminate round-off errors and use less memory. The dynamic relaxation method (DR) is one of the powerful and simple explicit processes. The important point is that the DR does not require to store the global stiffness matrix, for which it just uses the residual loads vector. In this paper, a new approach to the DR method is expressed. In this approach, the damping, mass and time steps are similar to those of the traditional method of dynamic relaxation. The difference of this proposed method is focused on the method of calculating the damping. The proposed method is expressed such that the time step is constant, damping is equal to zero except in steps with maximum energy and the concentrated damping can be applied to minimize the energy of system in this step. In this condition, the calculation of damping in all steps is not required. Then the volume of computation is reduced. The DR method for form-finding of membrane structures is employed in this paper. The form-finding of the three plans related to the membrane structures with different loading is considered to investigate the efficiency of the proposed method. The numerical results show that the convergence rate based on the proposed method increases in all cases than other methods.

Keywords: dynamic relaxation method; concentrated damping; form-finding; membrane structures

1. Introduction

Solving system of equations for analysis of every structure is necessary. For this purpose, two ways are available. One of them is repetitive method that is used for linear or nonlinear analysis of structures. Dynamic relaxation method (DR) is one of these iterative methods. The DR is used for analysis of static and dynamic systems. In DR, static systems are converted to artificial dynamic

∗Corresponding author, Associate Professor, E-mail: tkang@snu.ac.kr
[a]Former Master's Student, E-mail: sf.labbafi@yahoo.com
[b]Assistant Professor, E-mail: srsarafrazi@birjand.ac.ir
[c]Former Master's Student, E-mail: hgholami1369@gmail.com

http://www.techno-press.org/?journal=acd&subpage=7 ISSN: 2283-8477 (Print), 2466-0523 (Online)

systems by adding fictitious mass and damping forces to them. When masses and damping terms are selected properly, the responses of system converge to the static solutions.

The mathematical basis of Dynamic Relaxation method was rooted in the second order Richardson method that was proposed by Frankel (Frankel 1950). Since then, some other researchers (e.g., Otter 1966, Rushton 1969) have proposed variable methods for linear and nonlinear analysis by DR and improved it. This method was utilized for solving linear and nonlinear structural problems. The stability conditions of frame structures in DR were studied, and DR was formulated by Brew and Brotton (1971). The convergence rate of DR was increased by defining fictitious mass (Wood 1971, 2002), and then critical damping was estimated by Bunce (1972). The fictitious mass value and application of this for nonlinear problems was introduced using Geershgorin theory (Cassell and Hobbs 1976) by Cundall (1976). By deleting damping factor from the DR procedure, a new method was proposed in 1976 (Cundall 1976). This new DR was named Kinetic damping that was further improved in 2008 (Topping and Ivanyi 2008). Also, the DR method was used for nonlinear analysis of plates (Frieze *et al.* 1978). The Frist analysis of error in DR was done in 1981, and an automatic procedure for selection of their parameters was introduced by Papadrakakis (1981). The common formulation of DR was proposed by Underwood (1983). The DR was used for form-finding of pre-stressed membrane structures and for the finite element analysis of plate bending, which were studied in 1987 and 1988 by Al-Shawi and Mardirosian (1987) and Barnes (1988), respectively. After these studies, many other ways for calculating fictitious parameters of DR were proposed (Qiang 1988, Zhang and Yu 1989, Zhang *et al.* 1994, Rezaiee-Pajand and Taghavian Hakkak 2006, Kadkhodayan *et al.* 2008, Rezaiee-Pajand and Alamatian 2010, Rezaiee-Pajand *et al.* 2011, Rezaiee-Pajand and Sarafrazi 2010, 2011, Alamatian 2012). Regarding the form-finding of membrane structures, previous studies were done that are briefly stated below.

The form-finding is a process of finding the basic static shape of the structure taking into account pre-tension forces only. It is done before a detailed analysis, involving imposed loads such as snow and wind loads (Lewis 2003, Xu *et al.* 2015, Gil Pérez *et al.* 2016, 2017). Barnes (1988) discussed about Kinetic damping of DR in form-finding of pre-stressed membrane roofs. Wood (2002) presented a simple technique for controlling mesh in the process of the form-finding of membrane structures using DR method. Recently, Bagrianski and Halpern (2014) presented a new DR method for the form-finding of compressive structures. Veenenedaal and Block (2012) compared existing form-finding methods such as stiffness matrix, force density, surface stress density and DR method in form-finding of fabric structures (Veenendaal *et al.* 2011). Also, Veenendaal and Block (2012) studied these methods in form-finding of discrete networks. Nabaei *et al*. (2013) proposed form-finding procedure using a newly modified DR method for the form-finding of timber fabric structures. Very recently, Labbafi *et al*. (2017) studied the best method among five viscous and kinetic dynamic relaxation methods in form-finding of membrane structures. They investigated the rate of convergence is increased the most by considering the damping and mass in the algorithms proposed by Rezaiee-Pajand and Alamatian (2010).

In this paper, a new approach for damping factor in dynamic relaxation process is used for formulating concentrated damping that has not been used. As such, formulation of concentrated damping (C-damping) and steps of this method are proposed. To demonstrate the new features of this approach, several membrane structures are studied. Three different models of membrane structures of flat stretched membrane, spherical cap membrane, and triangular stretched membrane are investigated.

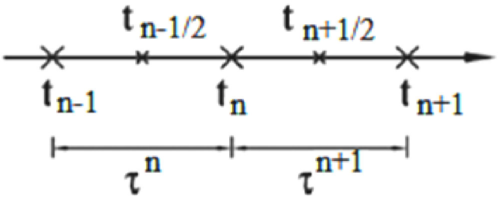

Fig. 1 Variable time step in successive DR iterations

2. Overview of dynamic relaxation method

2.1 Popular damping method

The idea of Dynamic Relaxation method is to add fictitious inertial and damping forces into a static system of equations and transfer it to a dynamic system as below (Rezaiee-Pajand and Rezaee 2014)

$$\mathbf{M}\ddot{\mathbf{X}} + \mathbf{C}\dot{\mathbf{X}} + \mathbf{S}\mathbf{X} = \mathbf{P} \tag{1}$$

where $\mathbf{X}$, $\dot{\mathbf{X}}$ and $\ddot{\mathbf{X}}$ are the vectors of displacement, velocity and acceleration, respectively. In addition, **M** is the fictitious mass matrix, **C** is the fictitious damping matrix, **K** is the stiffness matrix, and **P** is the external force vector.

For the formulation of a dynamic relaxation, numerical techniques are used. According to the form, the velocity and acceleration vectors can be written as follows

$$\dot{\mathbf{X}}^{n+½} = \frac{1}{\tau^{n+1}}\left(\mathbf{X}^{n+1} - \mathbf{X}^{n}\right) \tag{2}$$

$$\dot{\mathbf{X}}^{n} = \frac{1}{2}\left(\dot{\mathbf{X}}^{n-½} + \dot{\mathbf{X}}^{n+½}\right) \tag{3}$$

$$\ddot{\mathbf{X}}^{n} = \frac{1}{\tau^{n}}\left(\dot{\mathbf{X}}^{n+½} - \dot{\mathbf{X}}^{n-½}\right) \tag{4}$$

where is the time step and *n* is the iteration of DR method. By using Eqs. (2) to (4) and plugging them into dynamic system (Eq. (1)), the main formulations of DR are obtained as below

$$\mathbf{X}^{n+1} = \mathbf{X}^{n} + \tau^{n+1}\dot{\mathbf{X}}^{n+1/2} \tag{5}$$

$$\begin{aligned} \dot{\mathbf{X}}^{n+1/2} &= \frac{2-\tau^n c^n}{2+\tau^n c^n}\dot{\mathbf{X}}^{n-1/2} + \frac{2\tau^n}{2+\tau^n c^n}\mathbf{M}^{-1}\mathbf{R}^n \\ &= \frac{2-\tau^n c^n}{2+\tau^n c^n}\dot{\mathbf{X}}^{n-1/2} + \frac{2\tau^n}{2+\tau^n c^n}\left\{\frac{\mathrm{R}_i}{\mathrm{m}_{ii}}\right\}^n \end{aligned} \tag{6}$$

In these equations, m^n_{ii} and r^n_i are the i-th diagonal element of mass matrix and the residual force for i-th degree of freedom, respectively. The residual force in n-th step is calculated by the vectors of $\mathbf{P}$ and $\mathbf{f}$ that represent the external and internal forces, respectively, as shown below

$$\mathbf{R}^n = \mathbf{P}^n - \mathbf{f}^n \tag{7}$$

Typically, the damping matrix is defined as a multiple of the mass matrix. This equation of damping can be written as $\mathbf{C} = c\mathbf{M}$, where c is the damping factor that is used in Eq. (6).

In the DR process, fictitious mass, damping factor and time step are unknown. In common approaches, Gerschgorin's theory and Rayleigh's principle are used for mass matrix and damping factor, respectively (Cassell and Hobbs 1976). Also, in many DR methods, the time step is constant and equal to one.

For the i-th diagonal element of the mass matrix and critical damping, the below formulation can be used

$$\mathrm{m}_{ii} = \frac{\left(\tau^n\right)^2}{4} \sum_{i=1}^{ndof} \left|\mathrm{S}_{ij}\right| \tag{8}$$

$$c^n = 2\sqrt{\frac{\left(\mathbf{X}^n\right)^T \mathbf{f}\left(\mathbf{X}^n\right)}{\left(\mathbf{X}^n\right)^T \mathbf{M}\mathbf{X}^n}} \tag{9}$$

where *ndof* is the number of degrees of freedoms and *S* is the stiffness matrix.

2.2 Kinetic damping method

The Kinetic damping method is one of the DR methods that do not require calculating the damping factor in the DR process. The initial idea for Kinetic damping was suggested by Cundall (1976) for analyzing unstable rock mechanics problems and then it was impoved by Topping and Ivanyi (2008). The deletion of damping factor reduces volume of calculations, and time step and mass matrix are unknown. In this method, Eq. (8) is used for the calculation of mass matrix and time step is constant as other methods.

In Kinetic damping, no damping factor is used. The kinetic energy of a complete structure is traced as the undamped oscillations proceed, and all current nodal velocities are reset to zero whenever an energy peak is detected. Then the velocities in (n+1/2) is recalculated by the below formula

$$\dot{\mathbf{X}}^{n+1/2} = \frac{\tau}{2\mathbf{M}} \mathbf{R}^n \tag{10}$$

where $\mathbf{R}^n$ is the residual forces and is calculated from $\mathbf{X}^{n-1/2}$, as shown below

$$\mathbf{X}^{n-1/2} = \mathbf{X}^{n+1} - \frac{3\tau\dot{\mathbf{X}}^{n+1/2}}{2} + \frac{\tau^2\mathbf{R}^n}{2\mathbf{M}} \tag{11}$$

3. Proposed method

The process of DR is started by assuming an initial solution. The next steps are done in such a way that the residual forces are decreased. The proper value of fictitious mass and time step guarantees the convergence of the proposed DR procedure. On the other hand, the convergence rate is dependent upon the value of damping factor, which is calculated using the lowest eigenvalue of artificial dynamic system in the common dynamic relaxation method. The convergence of the DR method with zero damping factor is achieved utilizing Kinetic damping. In the Kinetic dynamic relaxation process, the velocities of the joints are set to zero when a fall in the level of total kinetic energy of the structure occurs. However, it is difficult to calculate the extreme point of kinetic energy. Topping and Ivanyi (2008) suggested assuming the peak point at the mid-point of the previous time-step when a fall down in kinetic energy occurs. The time-step ratio can be calculated in such a way that the responses converge to exact solutions.

In this proposed method, the time step is constant and equal to one, and the damping is equal to zero except in steps with maximum energy. Thus the concentrated damping can be applied to minimize the energy of system just in this step. The kinetic energy of the system is given by the following

$$\mathrm{U} = \frac{1}{2}\dot{\mathbf{X}}^T\mathbf{M}\dot{\mathbf{X}} \tag{12}$$

With replacement of the values of velocity in the energy equation and its derivative with respect to damping, the following equation is obtained

$$\frac{dU}{dc} = \frac{d}{dc}\dot{\mathbf{X}}^T\mathbf{M}\ddot{\mathbf{X}} = \sum_{i=1}^{ndof}\frac{d}{dc}\dot{\mathrm{X}}_{\mathrm{i}}\mathrm{m}_{\mathrm{ii}}\dot{\mathrm{X}}_{\mathrm{i}} = 0 \tag{13}$$

$$\sum_{i=1}^{ndof}\mathrm{m}_{\mathrm{ii}}\left(\frac{2-c\tau}{2+c\tau}\dot{\mathrm{X}}_i^{n-\frac{1}{2}} + \frac{2\tau}{2+c\tau}\mathrm{R}_i^n\mathrm{m}_{ii}^{-1}\right)\left(\frac{-4\tau}{\left(2+c\tau\right)^2}\dot{\mathrm{X}}_i^{n-\frac{1}{2}} - \frac{2t}{\left(2+c\tau\right)^2}\mathrm{R}_i^n\mathrm{m}_{ii}^{-1}\right) = 0 \tag{14}$$

One of the answers of the above equation is obtained as follows

$$\tau\dot{\mathbf{X}}^{n-\frac{1}{2}}c = 2\dot{\mathbf{X}}^{n-\frac{1}{2}} + 2\tau\mathbf{M}^{-1}\mathbf{R}^n \tag{15}$$

$$c = \frac{\left(\mathbf{A}\right)^T\mathbf{B}}{\left(\mathbf{A}\right)^T\mathbf{A}} \tag{16}$$

where,

$$\mathbf{A} = \tau\dot{\mathbf{X}}^{n-\frac{1}{2}} \tag{17}$$

$$\mathbf{B} = 2\dot{\mathbf{X}}^{n-\frac{1}{2}} + 2\tau\mathbf{M}^{-1}\mathbf{R}^n \tag{18}$$

The calculation of damping just in some of steps is the main difference of this method from the traditional method. Thus, the volume of computation is reduced. Also, the above method does not require calculating the residual forces in the middle of steps as in Kinetic damping. Therefore, a large amount of calculation of the Dynamic Relaxation process is eliminated. To verify the proposed method and the number of iterations to converge, numerical examples are considered in

Section 5, *Numerical examples*.

The algorithm for the proposed method is given as follows:

1. Define $\varepsilon_r, \mathbf{X}^0, \dot{\mathbf{X}}^{-1/2} = 0$.
2. $n = 1$.
3. Assembling the internal force vector and applying boundary conditions.
4. Evaluating the residual forces, stiffness matrix and artificial mass matrix.
5. Determine $\dot{\mathbf{X}}^{n+1/2}$ and $\mathbf{X}^{n+1}$.
6. Calculating energy (E_n).
7. If $E_{n-1} < E_n$, continue the iteration from step (3).
8. Evaluating damping factor from Eq. (16).
9. Recalculating $\mathbf{X}^{n+1}$, $\dot{\mathbf{X}}^{n+1/2}$ and E_n.
10. If $\|\mathbf{R}^{n+1}\| \le \varepsilon_r$ then stop the algorithm.
11. $n = n + 1$.
12. If $n < N_{max}$, continue from step (3).

Here, N_{max} is the maximum allowable number of iterations, which should be defined by the analyst, and ε_r is the maximum allowable error of displacement.

4. Required formulation for form-finding of membrane structures

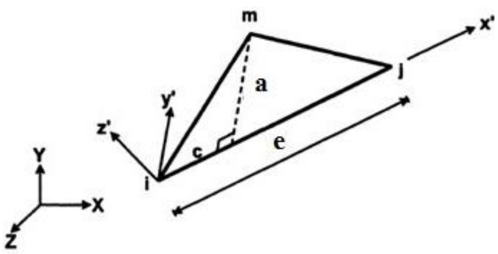

Fig. 2 Triangular finite element in its local coordinate system (Spillers *et al.* 1992, Levy and Spillers 2003)

The simplest finite element, the triangular plane stress (constant stress) element, is used. In the element, the node equilibrium equations appear in the local coordinate system (Spillers *et al.* 1992, Levy and Spillers 2003) (see Fig. 2).

$$\mathbf{F}^e = \frac{\mathrm{t}}{2}\begin{Bmatrix} b_\mathrm{i}\sigma_x + c_i\tau_{xy} \\ c_i\sigma_y + b_\mathrm{i}\tau_{xy} \\ \vdots \\ b_\mathrm{j}\sigma_x + c_\mathrm{j}\tau_{xy} \\ c_\mathrm{j}\sigma_y + b_\mathrm{j}\tau_{xy} \\ \vdots \\ b_\mathrm{m}\sigma_x + c_\mathrm{m}\tau_{xy} \\ c_\mathrm{m}\sigma_x + b_\mathrm{m}\tau_{xy} \end{Bmatrix} = \frac{\mathrm{t}}{2}\begin{Bmatrix} (\mathbf{F}_i)_x \\ (\mathbf{F}_i)_y \\ \vdots \\ (\mathbf{F}_j)_x \\ (\mathbf{F}_j)_y \\ \vdots \\ (\mathbf{F}_m)_x \\ (\mathbf{F}_m)_y \end{Bmatrix} \tag{19}$$

Here, σ_x, σ_y and τ are the usual stresses of plane elasticity, t is thickness of membrane, and b and c are the coefficients defined below. The gradient of Eq. (19) has the following particular simple form

$$\mathbf{K}_G^e = \begin{bmatrix} 0 & \mathbf{A} & \text{-}\mathbf{A} \\ \text{-}\mathbf{A} & 0 & \mathbf{A} \\ \mathbf{A} & \text{-}\mathbf{A} & 0 \end{bmatrix} \tag{20}$$

where,

$$\mathbf{A} = \frac{\mathrm{t}}{2}\begin{bmatrix} -\tau_{xy} & \sigma_x \\ -\sigma_y & \tau_{xy} \end{bmatrix} \tag{21}$$

The gradient in Eq. (20) is taken with respect to the node coordinates x_i, y_i, …, while holding the stress of σ_x, σ_y and τ fixed. To do so, it is required to define the coefficients used in Eq. (19), which are typically given as

$$b_i = y_i - y_m,\ c_i = x_m - x_j,\ \ldots \tag{22}$$

For completeness, the plane stress elastic stiffness matrix for the system is given as

$$\mathbf{K}_{2D}^e = \begin{bmatrix} (\mathbf{K}_{2D}^e)_{\mathrm{ii}} & (\mathbf{K}_{2D}^e)_{\mathrm{ij}} & (\mathbf{K}_{2D}^e)_{\mathrm{im}} \\ (\mathbf{K}_{2D}^e)_{\mathrm{ji}} & (\mathbf{K}_{2D}^e)_{\mathrm{jj}} & (\mathbf{K}_{2D}^e)_{\mathrm{jm}} \\ (\mathbf{K}_{2D}^e)_{\mathrm{mi}} & (\mathbf{K}_{2D}^e)_{\mathrm{mj}} & (\mathbf{K}_{2D}^e)_{\mathrm{mm}} \end{bmatrix} \tag{23}$$

where,

$$(\mathbf{K}_{2D}^e)_{\mathrm{rs}} = \frac{1}{4A}\frac{E}{1-\nu^2}\begin{bmatrix} b_{\mathrm{r}}b_{\mathrm{s}} + \frac{1-\nu}{2}c_{\mathrm{r}}c_{\mathrm{s}} & \nu b_{\mathrm{r}}b_{\mathrm{s}} + \frac{1-\nu}{2}c_{\mathrm{r}}b_{\mathrm{s}} \\ \nu b_{\mathrm{r}}b_{\mathrm{s}} + \frac{1-\nu}{2}b_{\mathrm{r}}c_{\mathrm{s}} & c_{\mathrm{r}}c_{\mathrm{s}} + \frac{1-\nu}{2}b_{\mathrm{r}}b_{\mathrm{s}} \end{bmatrix} \quad \mathrm{r,s = i,j,m} \tag{24}$$

Here, E and ν are the Young's modulus and Poisson's ratio, respectively, and A is the surface area of the triangular finite element. An additional step is required to deal with three dimensional membranes using the stiffness matrix (K_G^*) for 3D as follows

$$\mathbf{K}_G^{e\,*} = \frac{\mathrm{t}}{2}\begin{bmatrix} \mathbf{K}_{G\ \mathrm{ii}}^{e\,*} & \mathbf{K}_{G\ \mathrm{ij}}^{e\,*} & \mathbf{K}_{G\ \mathrm{mi}}^{e\,*} \\ \mathbf{K}_{G\ \mathrm{ij}}^{e\,*} & \mathbf{K}_{G\ \mathrm{jj}}^{e\,*} & \mathbf{K}_{G\ \mathrm{mj}}^{e\,*} \\ \mathbf{K}_{G\ \mathrm{im}}^{e\,*} & \mathbf{K}_{G\ \mathrm{jm}}^{e\,*} & \mathbf{K}_{G\ \mathrm{mm}}^{e\,*} \end{bmatrix} \tag{25}$$

$$\mathbf{K}_{Gir}^{e\ *} = \begin{bmatrix} 0 & 0 & 0 \\ 0 & 0 & 0 \\ 0 & 0 & \alpha_r \end{bmatrix};\ \mathbf{K}_{Gjr}^{e\ *} = \begin{bmatrix} 0 & 0 & 0 \\ 0 & 0 & 0 \\ 0 & 0 & \beta_r \end{bmatrix};\ \mathbf{K}_{Gmr}^{e\ *} = \begin{bmatrix} 0 & 0 & 0 \\ 0 & 0 & 0 \\ 0 & 0 & \lambda_r \end{bmatrix} \tag{26}$$

$$a_r = -\frac{e-c}{ae}(\mathbf{F}_r)_{y'} - \frac{1}{e}(\mathbf{F}_r)_{x'} \quad ; \quad r = i, j, m \tag{27}$$

$$\beta_r = -\frac{c}{ae}(\mathbf{F}_r)_{y'} = +\frac{1}{e}(\mathbf{F}_r)_{x'} \quad ; \quad r = i, j, m \tag{28}$$

$$\lambda_r = -\frac{1}{a}(\mathbf{F}_r)_{y'} \quad ; \quad r = i, j, m \tag{29}$$

5. Numerical examples

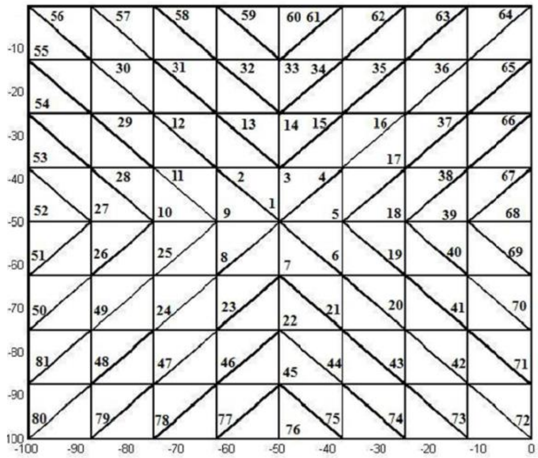

Fig. 3 Flat stretched membrane (Levy and Spillers 2003) (Units: in.; Conversion: 1 in. = 25.4 mm) (Numbering is shown)

Table 1 Cases for form-finding of spherical cap

Case	Type of loading	Load (kN)	Pre-tension force (MPa)	Location of applied force
1	First loading	44.482 kN	551.72	Center of the membrane
2	Second loading	44.482 kN	551.72	All internal nodes
3	Third loading	0.4448 kN	5.517	Two mid-points of the plan

To study the efficiency of the proposed method in form-finding of membrane structures, seven different schemes summarized in the preceding Section 2, *Overview of Dynamic Relaxation method*, and Section 3, *Proposed method*, are considered. Geometrically nonlinear analysis is programmed to analyze these schemes. The initial value of the time step in the DR method procedures is set equal to 1. The acceptable residual errors are the same for all solutions and are equal to 10^{-4}. Also, the total number of iterations and the analysis durations are recorded for each case. These schemes have the same accuracy. However, they require the different number of iterations to achieve the desired accuracy.

5.1 Flat stretched membrane

Fig. 3 shows a plan view of the analysis model. This model has 81 nodes that are subject to three different loadings. The Young's modulus is 10,000 ksi (68,950 MPa) and Poisson's ratio is 0.3. The pre-tension forces in x and y directions are 80,000 psi (551.72 MPa) for all different loadings of this example. Characteristics of different cases are summarized in Table 1.

5.1.1 Flat stretched membrane, Case 1

For the first loading, a concentrated load of 10,000 lb (44.482 kN) is applied at the center of the membrane. The results of analysis of Case 1 are shown in Table 2. The proposed method in this case has a very good performance. The form-finding shape and load displacement curve of this case are shown in Figs. 4 and 5, respectively.

Table 2 Results of analysis for form-finding of stretched membrane, Case 1

Case	Method of analysis	Number of iterations	CPU time (sec)
	DR	1312	8.11
1	Kinetic DR	2019	9.92
	Proposed method	428	2

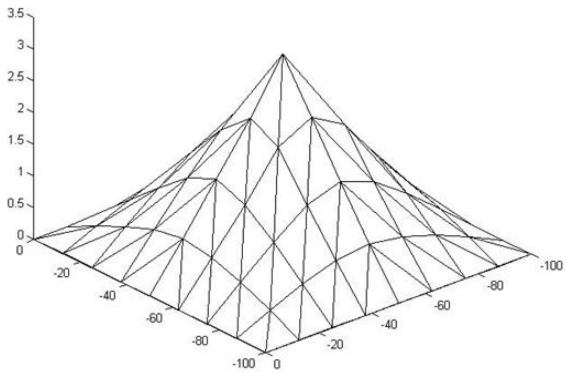

Fig. 4 Form-finding of flat stretched membrane in Case 1 (Units: in.; Conversion: 1 in. = 25.4 mm)

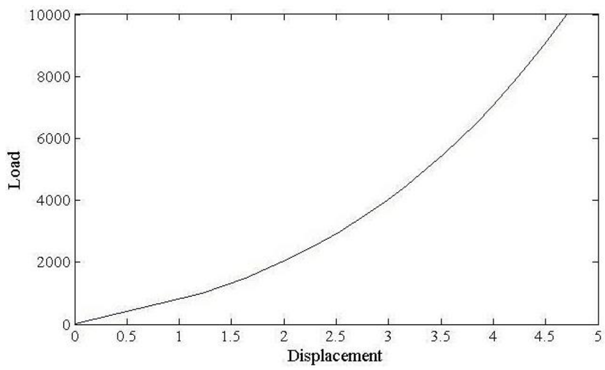

Fig. 5 Load-displacement curve for flat stretched membrane in Case 1 (Load in lb and Displacement in in.; Conversion: 1 lb = 4.448 N and 1 in. = 25.4 mm)

5.1.2 Flat stretched membrane, Case 2

For the second loading of flat stretched membrane, the forces of 10,000 lb (44.482 kN) are distributed over all internal nodes. The shapes of all four support sides are parabolic with different height. The results of analysis of Case 2 are shown in Table 3 and Figs. 6 and 7. The proposed method in this case reduces the number of iteritions and CPU time compared to the other methods.

Table 3 Results of analysis for form-finding of stretched membrane, Case 2

Case	Method of analysis	*Number* of iterations	CPU time (sec)
	DR	1252	9.30
2	Kinetic DR	1681	11
	Proposed method	4	7.68

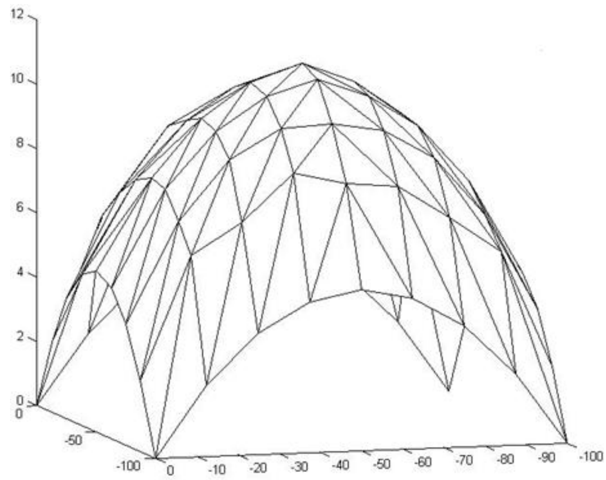

Fig. 6 Form-finding of flat stretched membrane in Case 2 (Units: in.; Conversion: 1 in. = 25.4 mm)

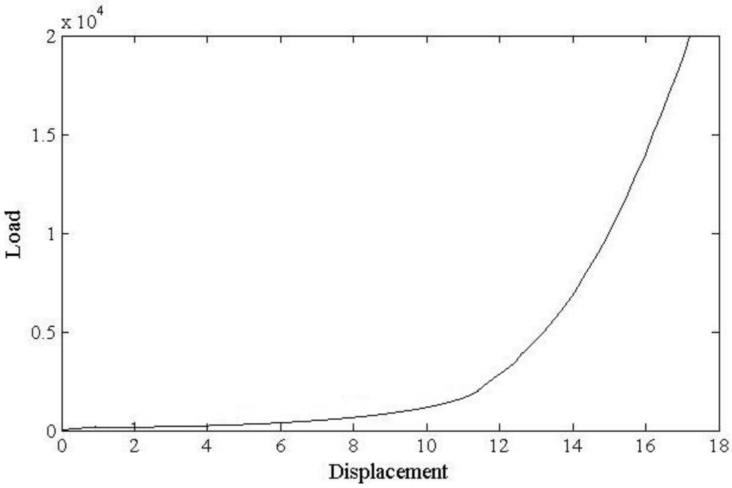

Fig. 7 Load-displacement curve for flat stretched membrane in Case 2 (Load in lb and Displacement in in.; Conversion: 1 lb = 4.448 N and 1 in. = 25.4 mm)

5.1.3 Flat stretched membrane, Case 3

Finally for the third loading in flat stretched membrane, only two mid-points of the plan are subject to concentrated loads of 50 lb (0.22241 kN) for each point. From Table 4, the proposed method has better performance than the DR method and Kinetic DR method, as the number of iterations and CPU time are 155 and 1 sec, respectively (versus 412 or 912 and 3.25 or 6.5 sec). The 3D view of form-finding of this membrane is shown in Fig. 8. Fig. 9 presents the load-displacement curve for flat stretched membrane in Case 3.

Table 4 Results of analysis for form-finding of stretched membrane, Case 3

Case	Method of analysis	Number of iterations	CPU time (sec)
	DR	412	3.25
3	Kinetic DR	923	6.5
	Proposed method	155	1

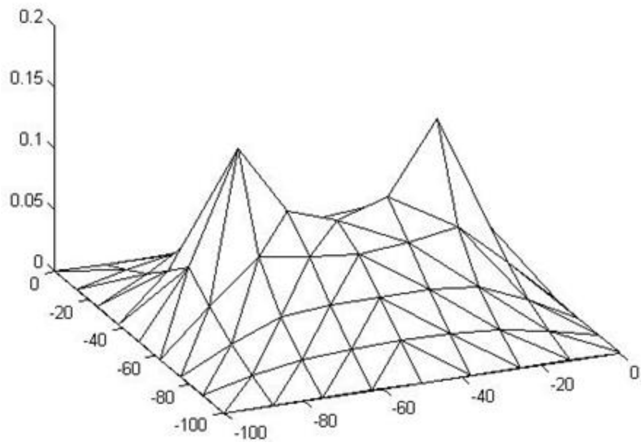

Fig. 8 Form-finding of flat stretched membrane in Case 3 (Units: in.; Conversion: 1 in. = 25.4 mm)

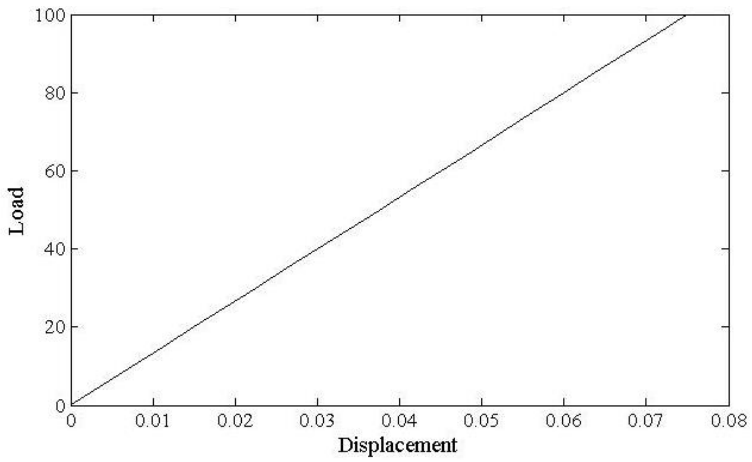

Fig. 9 Load-displacement curve for flat stretched membrane in Case 3 (Load in lb and Displacement in in.; Conversion: 1 lb = 4.448 N and 1 in. = 25.4 mm)

5.2 Spherical cap membrane

This example analyzes a spherical cap for membrane, which was also studied by Levy and Spillers (2003). Fig. 10 shows a plan view of the analysis model. The radius, thickness, Young's modulus and Poisson's ratio of this membrane are 0.9 in (22.86 mm), 0.01576 in (0.4 mm), 10,000 ksi (68,950 MPa) and 0.3, respectively. According to the Fig. 10, this model has 25 nodes that are subject to two different loadings that are described in Table 5. The pre-tension forces in x and y directions are 250,000 psi (1724.14 MPa) for this plan.

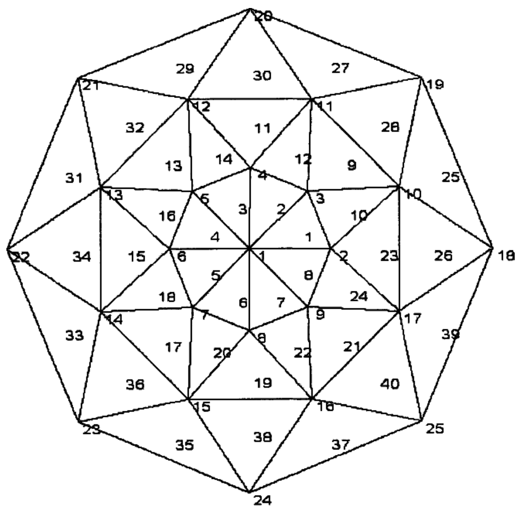

Fig. 10 Spherical membrane shell (Levy and Spillers 2003) (Numbering is shown)

Table 5 Cases for form-finding of stretched membrane

Case	Type of loading	Load (kN)	Pre-tension Force (MPa)	Location of applied force
1	First loading	44.48 kN	1724.14	node 1
2	Second loading	44.48 kN	1724.14	all internal nodes

5.2.1 Spherical cap membrane, Case 1

For the first loading, the load of 10,000 lb (44.48 kN) is applied at node 1, perpendicular to the plane of the membrane and in the positive direction. The number of iterations and the CPU time are listed in Table 6, showing reduction of iterations and time in the proposed method. The shapes of this loading and load displacement curve are shown in Figs. 11 and 12, respectively.

Table 6 Results of analysis for form-finding of spherical cap membrane, Case 1

Case	Method of analysis	Number of iterations	CPU time (sec)
	DR	363	0.6
1	Kinetic DR	1191	2.2
	Proposed method	194	0.5

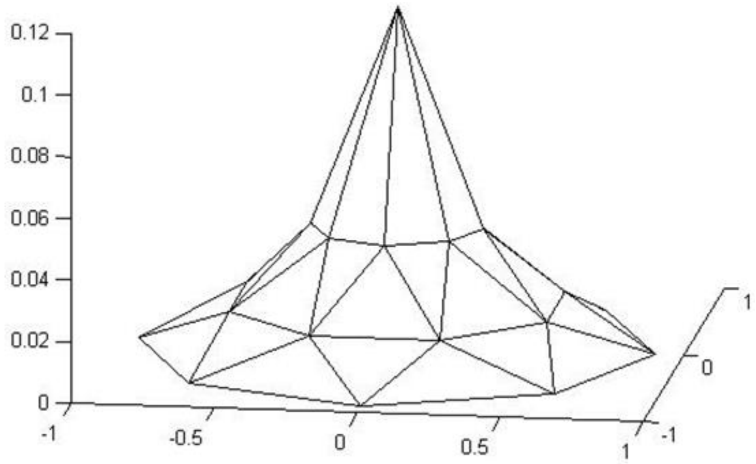

Fig. 11 Form-finding of spherical cap membrane in Case 1 (x-axis and y-axis have normalized dimensions)

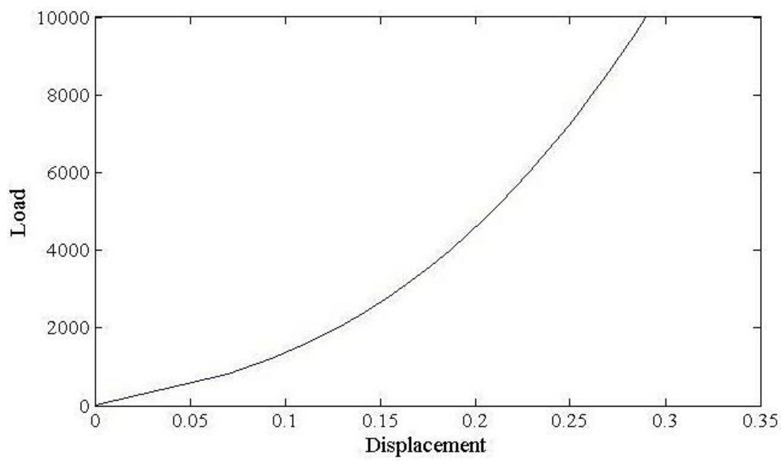

Fig. 12 Load-displacement curve for spherical cap membrane in Case 1 (Load in lb and Displacement in in.; Conversion: 1 lb = 4.448 N and 1 in. = 25.4 mm)

5.2.2 Spherical cap membrane, Case 2

For the second loaindg, the load of 10,000 lb (44.48 kN) is applied over all internal nodes. Table 7 and Figs. 13 and 14 show the results of analysis of the second loading in spherical cap membrane and the load-displacement curves. The CPU time in analysis is under 1 second for the proposed method and DR, with the former about half the latter

Table 7 Results of analysis for form-finding of Spherical cap membrane, Case 2

Case	Method of analysis	Number of iterations	CPU time (sec)
	DR	393	0.63
2	Kinetic DR	1418	2.5
	Proposed method	238	0.32

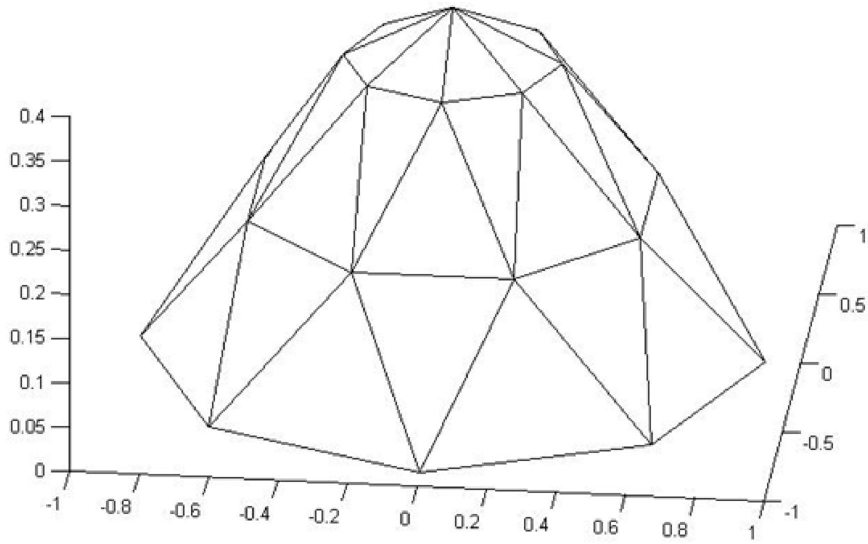

Fig. 13 Form-finding of spherical cap membrane in Case 2 (x-axis and y-axis have normalized dimensions)

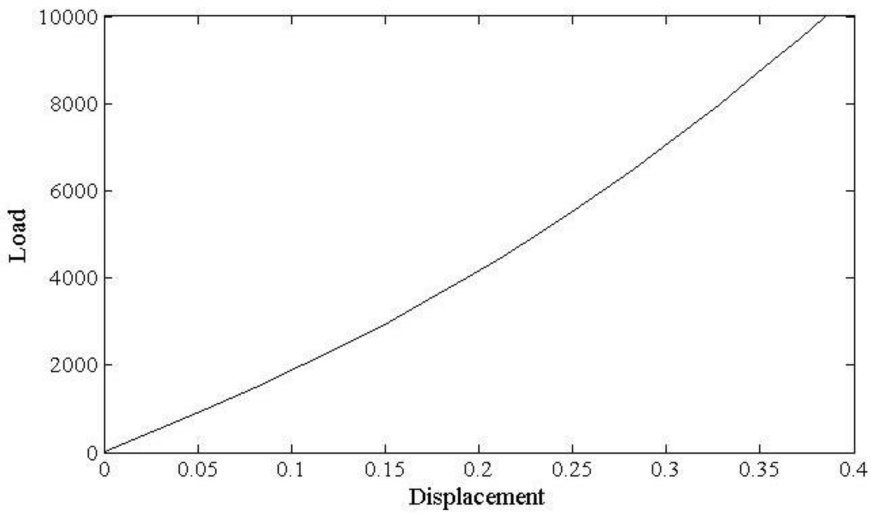

Fig. 14 Load-displacement curve for spherical cap membrane in Case 2 (Load in lb and Displacement in in.; Conversion: 1 lb = 4.448 N and 1 in. = 25.4 mm)

5.3 Triangular stretched membrane

In Fig. 15, a plan of equilateral triangle with sides of 160 in. (4,064 mm) is considered. This plan is created and loaded by the authors. According to the Fig. 15, this membrane has 66 nodes. Two cases of form-finding for this plan are achieved. The Young's modulus and Poisson's ratio are 10,000 ksi (68,950 MPa) and 0.3, respectively. The triangular stretched membrane has a thickness of 0.01576 in. (0.4 mm). The pre-tension forces in x and y directions are 300,000 psi (2068.95 MPa). Table 8 shows the value of loads and location of them in the two cases of triangular stretched membrane.

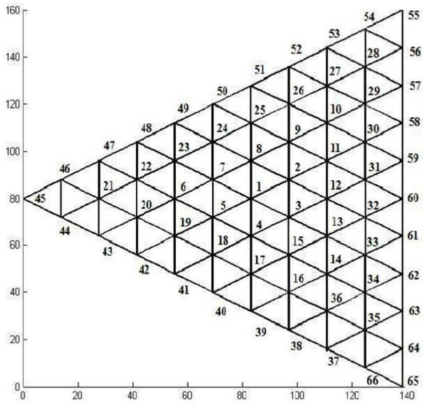

Fig. 15 Triangular stretched membrane (Units: in.; Conversion: 1 in. = 25.4 mm) (Numbering is shown)

Table 8 Cases for form-finding of spherical cap membrane

Case	Type of loading	Load (kN)	Pre-tension force (MPa)	Location of applied force
1	First loading	44.48 kN	2068.95	All internal nodes
2	Second loading	4.448 kN	2068.95	All internal nodes

5.3.1 Triangular stretched membrane, Case 1

For the first loading in triangular stretched membrane, the load of 10,000 lb (44.48 kN) is distributed over all internal nodes. The nodes on the sides of a triangle with unequal height are considered as a quadratic function. In this case, the proposed method has better performance than the DR method, as it reduces the number of iterations and time. Figs. 16 and 17 show the results of analysis for the first loading of triangular plan.

Table 9 Results of analysis for form-findingof triangular stretched membrane, Case 1

Case	Method of analysis	Number of iterations	CPU time (sec)
1	DR	656	3
	Kinetic DR	1908	8
	Proposed method	600	2.5

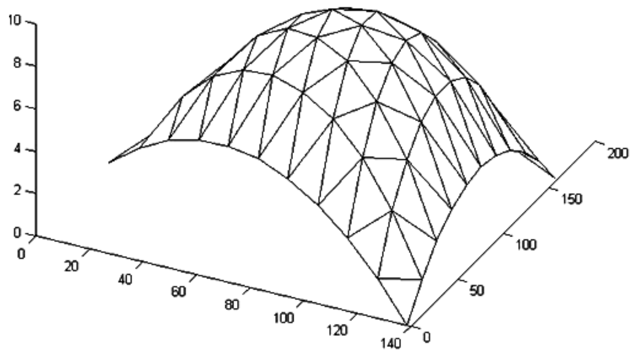

Fig. 16 Form-finding of triangular stretched membrane in Case 1 (Units: in.; Conversion: 1 in. = 25.4 mm)

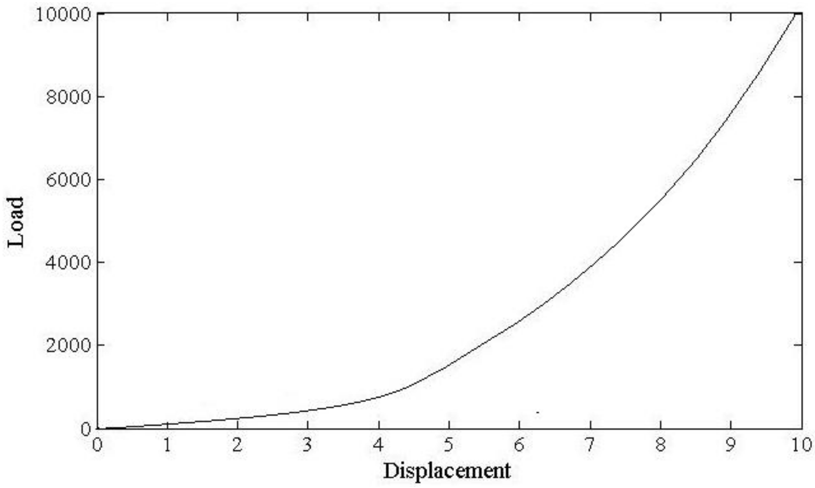

Fig. 17 Load-displacement curve for triangular stretched membrane in Case 1 (Load in lb and Displacement in in.; Conversion: 1 lb = 4.448 N and 1 in. = 25.4 mm)

5.3.2 Triangular stretched membrane, Case 2

In the second case, the load of 1,000 lb (4.448 kN) is applied at the center of the plan. The height of the membrane varies as a quadratic function. This case has less iterations by the proposed method, as shown in the results of analysis in Table 10.

Table 10 Results of analysis for form-finding of triangular stretched membrane, Case 2

Case	Method of analysis	Number of iterations	CPU time (sec)
2	DR	1537	6.8
	Kinetic DR	2474	8.7
	Proposed method	895	3.7

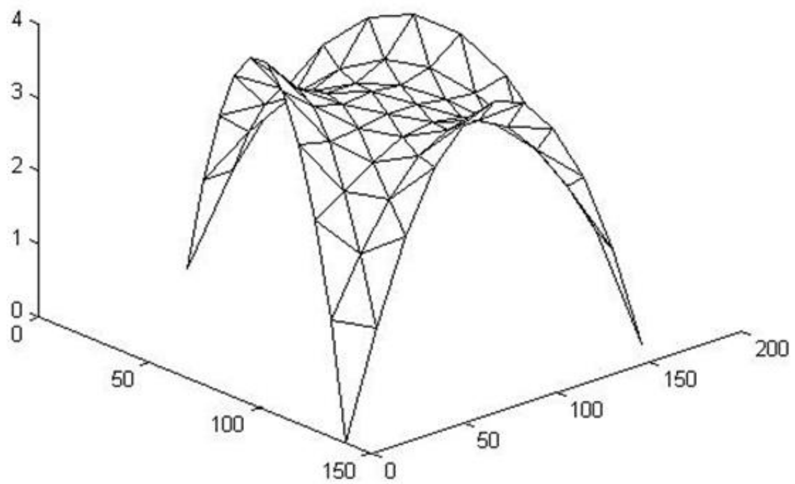

Fig. 18 Form-finding of triangular stretched membrane in Case 2 (Units: in.; Conversion: 1 in. = 25.4 mm)

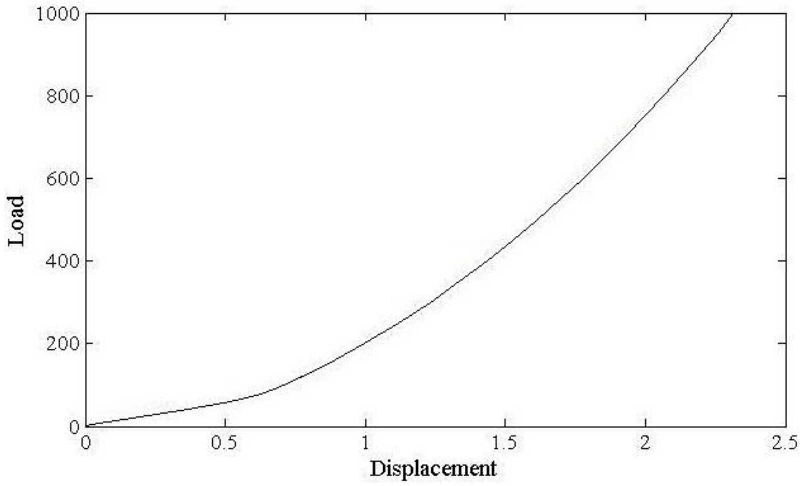

Fig. 19 Load-displacement curve for triangular stretched membrane in Case 2 (Load in lb and Displacement in in.; Conversion: 1 lb = 4.448 N and 1 in. = 25.4 mm)

6. Conclusions

In this paper, a comprehensive review of Dynamic Relaxation algorithms was conducted. Of these, the DR and Kinetic damping DR methods were described in detail. Then, the new Dynamic Relaxation algorithm was proposed. In this procedure, the artificial mass and time steps are similar to the DR methods. However, the damping factor is different from the DR methods. Damping factor is calculated only in some of specified steps. In other words, damping is zero in the most steps of the DR algorithm. Therefore, a total number of calculations is reduced. The concentrated damping is imposed, when the value of total kinetic energy of system is at its peak point. Utilizing the proper values of concentrated damping factors, the kinetic energy converges to zero. The presented formulation shows the relation between common and Kinetic Dynamic Relaxation processes, as well. It should be noted that the procedures of minimizing the kinetic energy by the proposed method and Topping and Ivanyi's algorithm are different. Topping and Ivanyi's kinetic technique requires more calculations. Finally, some representative membrane structures were selected for verification, and their geometric nonlinear analyses were performed. The numerical results show that the convergence rate of the proposed method significantly increases in all cases compared to the Kinetic damping and also popular damping used in the DR methods.

References

Alamatian, J. (2012), "A new formulation for fictitious mass of the dynamic relaxation method with kinetic damping", *Comput. Struct.*, **90**, 42-54.

Al-Shawi, F.A.N. and Mardirosian, A.H. (1987), "An improved dynamic relaxation method for the analysis of plate bending problems", *Comput. Struct.*, **27**(2), 237-240.

Bagrianski, S. and Halpern, A.B. (2014), "Form-finding of compressive structures using prescriptive dynamic relaxation", *Comput. Struct.*, **132**, 65-74.

Barnes, M.R. (1988), "Form-finding and analysis of prestressed nets and membranes", *Comput. Struct.*, **30**(3), 685-695.

Brew, J.S. and Brotton, D.M. (1971), "Non-linear structural analysis by dynamic relaxation", *Int. J. Numer. Meth. Eng.*, **3**(4), 463-483.

Bunce, J.W. (1972), "A note on the estimation of critical damping in dynamic relaxation", *Int. J. Numer. Meth. Eng.*, **4**(2), 301-303.

Cassell, A.C. and Hobbs, R.E. (1976), "Numerical stability of dynamic relaxation analysis of non-linear structures", *Int. J. Numer. Meth. Eng.*, **10**(6), 1407-1410.

Cundall, P.A. (1976), *Explicit Finite-Difference Method in Geomechanics*, Presented at the Numerical Methods in Geomechanics, Blacksburg, 132-150.

Frankel, S.P. (1950), "Convergence rates of iterative treatments of partial differential equations. Math", *Tab. Aid. Comput.*, **4**(30), 65-75.

Frieze, P.A., Hobbs, R.E. and Dowling, P.J. (1978), "Application of dynamic relaxation to the large deflection elasto-plastic analysis of plates", *Comput. Struct.*, **8**(2), 301-310.

Gil Pérez, M., Kang, T.H.K., Sin, I. and Kim, S.D. (2016), "Nonlinear design and analysis of membrane fabric structures: Modeling procedure and case studies", *ASCE J. Struct. Eng.*, 142.

Gil Pérez, M., Kim, S.D. and Kang, T.H.K. (2017), "Development of design aid for barrel vault shaped membrane fabric structures", *J. Struct. Integr. Mainten.*, **2**(1), 12-21.

Kadkhodayan, M., Alamatian, J. and Turvey, G.J. (2008), "A new fictitious time for the dynamic relaxation (DXDR) method", *Int. J. Numer. Meth. Eng.*, **74**(6), 996-1018.

Labbafi, S.F., Sarafrazi, S.R. and Kang, T.H.K. (2017), "Comparison of viscous and kinetic dynamic relaxation methods in form-finding of membrane structures", *Adv. Comput. Des.*, **2**(1), 71-87.

Levy, R. and Spillers, W.R. (2003), *Analysis of Geometrically Nonlinear Structures*, 2nd Edition, Springer, Dordrecht, New York, U.S.A.

Lewis, W.J. (2003), *Tension Structures: Form and Behaviour. Thomas Telford*.

Nabaei, S.S., Baverel, O. and Weinand, Y. (2013), "Mechanical form-finding of the timber fabric structures with dynamic relaxation method", *Int. J. Space Struct.*, **28**(3-4), 197-214.

Otter, J.R.H. (1966), "Dynamic relaxation compared with other iterative finite difference methods", *Nucl. Eng. Des.*, **3**(1), 183-185.

Papadrakakis, M. (1981), "A method for the automatic evaluation of the dynamic relaxation parameters", *Comput. Meth. Appl. Mech. Eng.*, **25**(1), 35-48.

Qiang, S. (1988), "An adaptive dynamic relaxation method for nonlinear problems", *Comput. Struct.*, **30**(4), 855-859.

Rezaiee-Pajand, M. and Alamatian, J. (2010), "The dynamic relaxation method using new formulation for fictitious mass and damping", *Struct. Eng. Mech.*, **34**.

Rezaiee-Pajand, M. and Taghavian Hakkak, M. (2006), "Nonlinear analysis of truss structures using dynamic relaxation(research note)", *Int. J. Eng.-Trans. B Appl.*, **19**, 11.

Rezaiee-Pajand, M., Kadkhodayan, M., Alamatian, J. and Zhang, L.C. (2011), "A new method of fictitious viscous damping determination for the dynamic relaxation method", *Comput. Struct.*, **89**(9), 783-794.

Rezaiee-Pajand, M. and Rezaee, H. (2014), "Fictitious time step for the kinetic dynamic relaxation method", *Mech. Adv. Mater. Struct.*, **21**(8), 631-644.

Rezaiee-Pajand, M. and Sarafrazi, S.R. (2010), "Nonlinear structural analysis using dynamic relaxation method with improved convergence rate", *Int. J. Comput. Meth.*, **7**(4), 627-654.

Rezaiee-Pajand, M. and Sarafrazi, S.R. (2011), "Nonlinear dynamic structural analysis using dynamic relaxation with zero damping", *Comput. Struct.*, **89**(13), 1274-1285.

Rushton, K.R. (1969), "Dynamic-relaxation solution for the large deflection of plates with specified boundary stresses", *J. Strain Anal. Eng. Des.*, **4**(2), 75-80.

Spillers, W.R., Schlogel, M. and Pilla, D. (1992), "A simple membrane finite element", *Comput. Struct.*, **45**(1), 181-183.

Topping, B.H.V. and Ivanyi, P. (2008), *Computer Aided Design of Cable Membrane Structures*, Saxe-Coburg Publications, Kippen, Stirlingshire, Scotland.

Underwood, P. (1983), *Dynamic Relaxation (in Structural Transient Analysis) Computational Methods for Transient Analysis*, Amsterdam, North-Holland, 245-265.

Veenendaal, D. and Block, P. (2012), "An overview and comparison of structural form finding methods for general networks", *Int. J. Sol. Struct.*, **49**(26), 3741-3753.
Veenendaal, D., West, M. and Block, P. (2011), "History and overview of fabric formwork: Using fabrics for concrete casting", *Struct. Concrete*, **12**(3), 164-177.
Wood, R.D. (2002), "A simple technique for controlling element distortion in dynamic relaxation form-finding of tension membranes", *Comput. Struct.*, **80**(27), 2115-2120.
Wood, W.L. (1971), "Note on dynamic relaxation", *Int. J. Numer. Meth. Eng.*, **3**(1), 145-147.
Xu, R., Li, D.X., Liu, W., Jiang, J.P., Liao, Y.H. and Wang, J. (2015), "Modified nonlinear force density method for form-finding of membrane SAR atenna", *Struct. Eng. Mech.*, **54**(6), 1045-1059.
Zhang, L.C., Kadkhodayan, M. and Mai, Y.W. (1994), "Development of the maDR method", *Comput. Struct.*, **52**(1), 1-8.
Zhang, L.G. and Yu, T.X. (1989), "Modified adaptive dynamic relaxation method and its application to elastic-plastic bending and wrinkling of circular plates", *Comput. Struct.*, **33**(2), 609-614.

CC